ACS OMEGA

Article

Cite This: ACS Omega 2020, 5, 243−251

http://pubs.acs.org/journal/acsodf

Synthesis and Evaluation of Artemisinin-Based Hybrid and Dimer Derivatives as Antimelanoma Agents

Lorenzo Botta,*[,†] Silvia Filippi,[†] Bruno M. Bizzarri,[†] Claudio Zippilli,[†] Roberta Meschini,[†] Rebecca Pogni,[‡] Maria Camilla Baratto,[‡] Luciano Villanova,[§] and Raffaele Saladino*[,†]

[†]Department of Ecological and Biological Sciences, University of Tuscia, via S. C. De Lellis 44, 01100, Viterbo, Italy

[‡]Department of Biotechnology, Chemistry and Pharmacy, University of Siena, via Aldo Moro 2, 53100 Siena, Italy

[§]Lachifarma s.r.l., S.S.16 Zona Industriale, 73010, Zollino, Lecce, Italy

Supporting Information

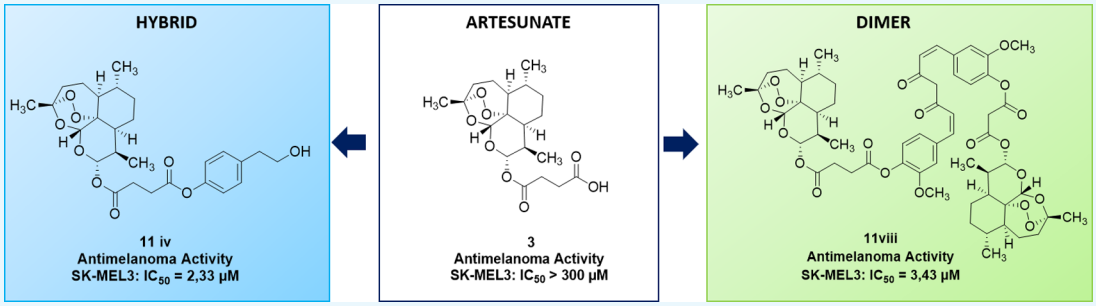

ABSTRACT: A library of hybrid and dimer compounds based on the natural scaffold of artemisinin was synthesized. These derivatives were obtained by coupling of artemisinin derivatives, artesunate, and dihydroartemisinin with a panel of phytochemical compounds. The novel artemisinin-based hybrids and dimers were evaluated for their anticancer activity on a cervical cancer cell line (HeLa) and on three complementary metastatic melanoma cancer cell lines (SK-MEL3, SK-MEL24, and RPMI-7951). Two hybrid compounds obtained by coupling of artesunate with eugenol and tyrosol, and one of the dimer compounds containing curcumin, emerged as the most active and cancer-selective derivatives.

INTRODUCTION

Artemisinin (**1**) is a sesquiterpene from *Artemisia annua* L. (sweet wormwood)[1] characterized by a reactive 1,2,4-trioxane ring (endoperoxide bridge) and a lactone moiety as pharmacophores (Figure 1).[2] This compound is applied in the treatment of different types of malaria.[3] Semisynthetic derivatives of artemisinin, dihydroartemisinin **2**, artesunate **3**, and artemether **4**, have been developed with the aim of increasing the pharmacological activity and the pharmacokinetic profile of the parent drug (Figure 1).[4] In addition, artemisinin and artemisinin derivatives showed remarkable activity against cancer cell lines,[5] including leukemia, melanoma, breast, ovarian, prostate, colon, and renal cancers, without inducing cytotoxicity in normal cells.[6] This selectivity is due to the iron-mediated cleavage of the endoperoxide bridge in tumor cells containing a higher concentration of this metal with respect to their normal cell counterpart.[7] Moreover, tumor cells usually show a diminished expression of antioxidant enzymes able to scavenge radical species.[8] Iron catalyzes the ring opening of the endoperoxide bridge of artemisinin, with subsequent generation of free-radical reactive oxygen and carbon-centered species,[9] followed by oxidative DNA damage. The mechanism is also responsible for the antimalarial effect of artemisinin, in which case the radical cascade is triggered by iron atoms delivered during the metabolic breakdown of hemoglobin in the vacuole of the parasite.[10]

Recently, the synthesis of hybrid and dimer derivatives of bioactive natural substances turned out to be a useful strategy to increase both biological activity and pharmacokinetic profiles, avoiding drug-resistance phenomena with respect to the individual starting compounds.[11] Dimers and hybrids of artemisinin and artemisinin derivatives in association with bioactive phytochemicals, such as thymoquinone, showed increased antileukemia and antimalarial activity.[12] Different dimers and hybrids of artemisinin derivatives containing natural phenol and catechol residues, such as 2-(3-hydroxyphenyl)ethanol and 3-hydroxytyrosol, have also been patented.[13]

We report here the synthesis of a novel library of artemisinin-based hybrid and dimer derivatives obtained by chemical coupling of dihydroartemisinin **2** and artesunate **3** with chemopreventive phytochemicals, including curcumin **5**, eugenol **6**, perillyl alcohol **7**, tyrosol **8**, α-tocopherol **9**, and δ-tocopherol **10**, respectively (Figure 1).[14] The products were evaluated on melanoma, the main cause of skin-cancer-related

Received: August 13, 2019
Accepted: October 15, 2019
Published: December 27, 2019

DOI: 10.1021/acsomega.9b02600
ACS Omega 2020, 5, 243−251

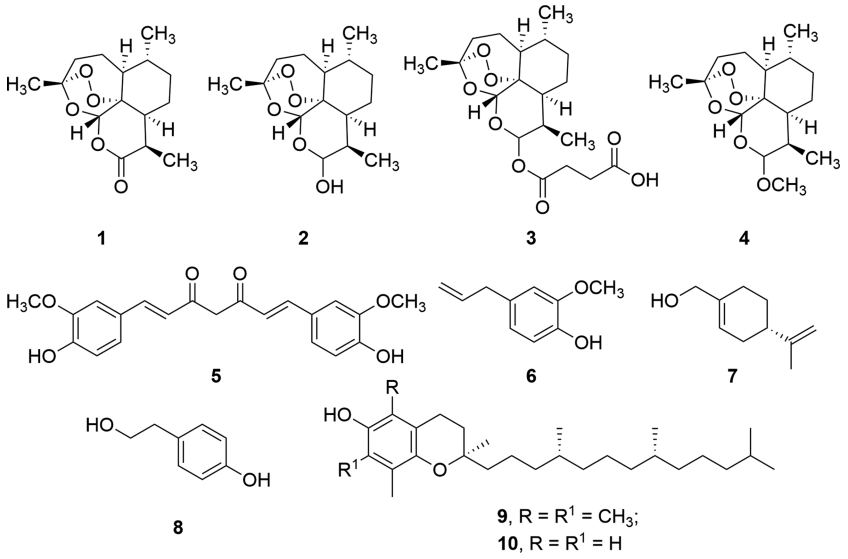

Figure 1. Artemisinin and semisynthetic derivatives of artemisinin and phytochemicals.

death and one of the most aggressive and lethal pathology in human.[15] In this context, phytochemicals **5**−**10** showed antimelanoma activity as isolated compounds or components of natural extracts.[16−19]

RESULTS AND DISCUSSION

Synthesis of Artemisinin-Based Hybrid and Dimer Derivatives. The hybrid derivatives of artemisinin, **11i**−**vi**, were synthesized by a procedure involving the reaction between artesunate **3** (1.0 mmol) and the appropriate phytochemical, **5**−**10** (1.1 mmol), in the presence of *N*,*N*′-dicyclohexylcarbodiimide (DCC) (1.2 mmol) and 4-dimethylaminopyridine (DMAP) (catalytic amount) as coupling agents (Scheme 1). Compounds **11i**−**vi** were obtained, as the only recovered products, besides the unreacted substrate, from acceptable to high yield (Table 1).

Scheme 1. Synthesis of Hybrid Derivatives 11i−iv

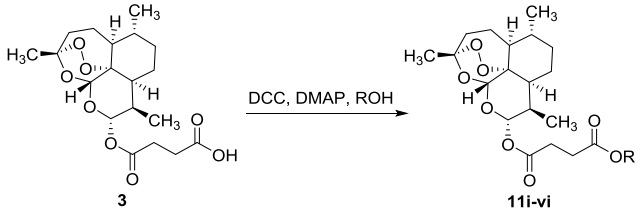

In addition, dimeric derivatives of artemisinin **11vii** and **11viii** were synthesized using phytochemicals bearing two reactive functional groups, such as curcumin **5** (two OH phenol moieties) and tyrosol **8** (OH phenol and primary alcohol moieties). In these latter cases, an excess of artesunate **3** (2.2 mmol) was required to optimize the yield of the desired product (Chart 1). Note that compound **11viii** was characterized by a C-2 internal symmetry property.

Finally, 4-hydroxyphenethyl bromide **12** was used as an electrophilic alkylating agent to obtain hybrid derivatives **11ix** and **11x** from artesunate **3** and dihydroartemisinin **2**, respectively (Scheme 2). The reactions were performed under general basic catalysis conditions (K_2CO_3) in dimethylformamide (DMF, 10 mL) at 90 °C.

Table 1. Yield of Hybrid Derivatives 11i−iv Obtained by the DCC/DMAP Coupling Reaction between Artesunate 3 and Phytochemicals 5−10[a,b]

Entry	R	Product	Yield (%)[b]
1	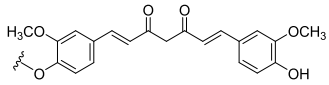	11i	50
2	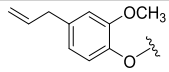	11ii	49
3	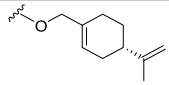	11iii	82
4	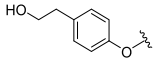	11iv	53
5	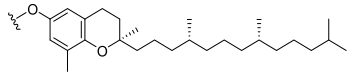	11v	72
6	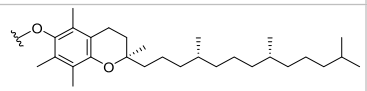	11vi	60

[a]The reactions were performed by treating artesunate **3** (1.0 mmol) with DCC (1.2 mmol), DMAP (catalytic amount), and the appropriate phytochemical, **5**−**10** (1.1 mmol), at 25 °C for 18h. [b]Experiments were conducted in triplicate.

In terms of structure relationships, compounds **11iv** and **11ix** were characterized by a different regioselectivity in the linkage of the tyrosol moiety to the artesunate scaffold, that is phenolic (**11iv**) versus primary alcohol (**11ix**) coupling site, respectively. The tyrosol moiety was linked to artesunate and dihydroartemisinin only by the primary alcoholic function in compounds **11ix** and **11x**.

DOI: 10.1021/acsomega.9b02600
ACS Omega 2020, 5, 243−251

Chart 1. Structures of Dimeric Derivatives 11vii and 11viii

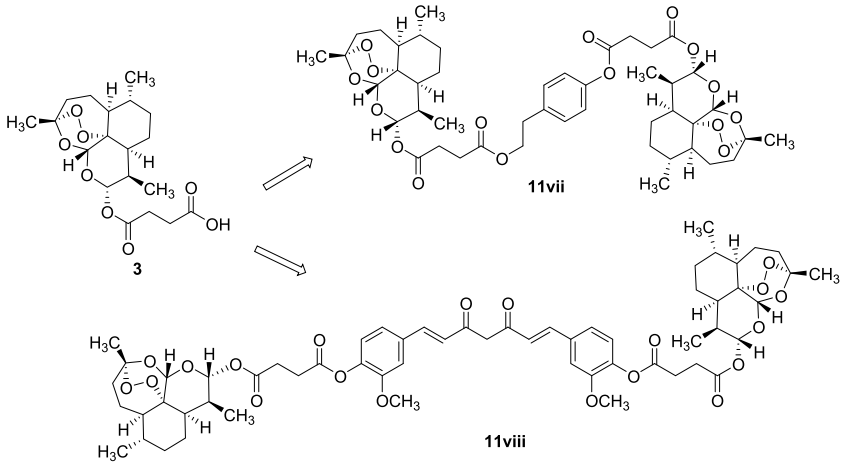

Scheme 2. Synthesis of Hybrid Derivatives 11ix (46%) and 11x (53%) from Artesunate 3 and Dihydroartemisinin 2, respectively

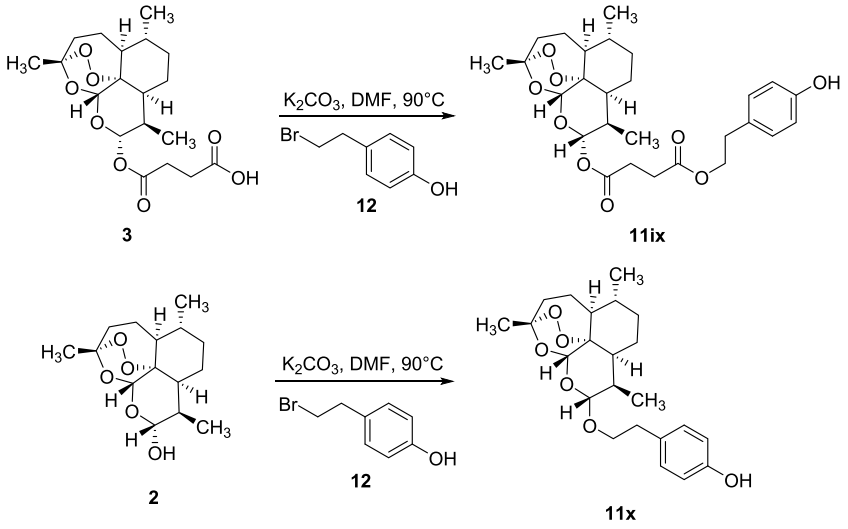

Biological Activity. Artemisinin derivatives can inhibit metastasis[20] and angiogenesis processes,[21] influencing some cancer-related signaling pathways.[22] We evaluated the anticancer activity of artemisinin **1**, dihydroartemisinin **2**, artesunate **3**, and artemisinin derivatives **11i–x** by cell survival [3-(4,5-dimethylthiazol-2-yl)-2,5-diphenyl-2H-tetrazolium bromide] (MTT) assay on a drug-resistant cervical cancer cell line (HeLa) and three complementary metastatic melanoma cancer cell lines, SK-MEL3, SK-MEL24, and RPMI-7951, respectively. The genetic characteristics of the SK-MEL3, SK-MEL24, and RPMI-7951 cell lines are summarized in Table 2. A normal human primary fibroblast cell line (C3PV) was used as a reference.

All three melanoma cell lines show the mutation of the B-RAF gene, which is involved in the regulation of the RAS/MAPK pathway, controlling cell proliferation, differentiation, migration, and apoptosis. The B-RAF gene mutation is highly frequent in both primary and metastatic melanoma cells, accounting for 50.9 and 66.3% of the total observed mutations, respectively.[23] Two cell lines, SK-MEL-3 and RPMI-7951, are mutated on the TP53 gene, which controls the synthesis of the p53 protein, involved in cell division and prevention of cancer formation.[24] Finally, the RPMI-7951 and SK-MEL24 cell lines were characterized by the cyclin-dependent kinase inhibitor 2A (CDKN2A)[25] and phosphatase and tensin homolog (PTEN)[26] gene mutations, controlling the production of tumor suppressor proteins.

Table 2. Genetic Properties of Melanoma Cancer Cell Lines Used in the Biological Evaluations

name	mutant gene[a]	zygosity[b]	gene Seq.[c]	protein seq[d]
SK-MEL3	BRAF	Heterozygous	c.1799T>A	p.V600E
	TP53	Homozygous	c.799 C>T	p.R267W
RPMI-7951	BRAF	Heterozygous	c.1799T>A	p.V600E
	CDKN2A	Homozygous	c.47T>G	p.L16R
	PTEN	Homozygous	c.1_79del79	
	TP53	Homozygous	c.497C>A	p.S166*
SK-MEL24	BRAF	Heterozygous	c.1799T>A	p.V600E
	CDKN2A	Homozygous	c.1_471del471	
	PTEN	Homozygous	c.80_164del85	

[a]These cell lines are characterized by mutations in different genes and gene regions that are representative of the metastatic melanoma. [b]Mutation state. [c]Mutation gene sequencing. [d]Mutation protein sequencing.

DOI: 10.1021/acsomega.9b02600
ACS Omega 2020, 5, 243−251

Table 3. Anticancer Activity of Artemisinin 1, Dihydroartemisinin 2, Artesunate 3, Hybrid Derivatives 11i-iv and 11ix-x, and Dimeric Derivatives 11vii and 11viii[a]

		$IC_{50} \pm SD$[b]				
entry	CPD	C3PV	HeLa	SK-MEL3	SK-MEL24	RPMI-7951
1	**1**	>300 ± 14.85	1.37 ± 0.59	3.43 ± 0.86	8.66 ± 4.56	3.62 ± 0.99
2	**2**	0.68 ± 0.19	1.32 ± 0.26	10.36 ± 0.61	3.23 ± 1.60	0.91 ± 0.45
3	**3**	1.68 ± 0.44	1.76 ± 0.38	>300 ± 5.07	0.82 ± 0.37	1.08 ± 0.56
4	**11i**	2.36 ± 0.24	1.15 ± 1.09	3.23 ± 0.37	5.88 ± 2.25	10.43 ± 1.60
5	**11ii**	6.79 ± 0.15	1.44 ± 1.09	4.65 ± 1.80	5.44 ± 2.4	1.21 ± 0.63
6	**11iii**	>300 ± 35.35	1.76 ± 0.47	5.24 ± 2.29	0.06 ± 0.1	2.35 ± 1.52
7	**11iv**	>300 ± 10.71	>300 ± 7.071	2.33 ± 1.18	2.32 ± 1.19	8.34 ± 3.06
8	**11v**	0.85 ± 0.32	4.39 ± 0.77	2.61 ± 0.49	>300 ± 21.21	3.06 ± 0.17
9	**11vi**	10.18 ± 1.57	3.34 ± 0.66	1.23 ± 0.83	3.69 ± 0.91	1.90 ± 0.35
10	**11vii**	6.10 ± 3.74	2.16 ± 0.54	32.78 ± 5.81	0.24 ± 0.12	0.49 ± 0.05
11	**11viii**	>300 ± 14.84	2.41 ± 0.56	3.43 ± 0.16	2.54 ± 0.47	1.37 ± 0.13
12	**11ix**	132.20 ± 12.58	2.66 ± 0.82	1.28 ± 0.15	1.5 ± 0.85	0.09 ± 0.03
13	**11x**	1.76 ± 0.31	2.73 ± 0.37	10.58 ± 1.14	3.01 ± 0.57	0.33 ± 0.08
14	**5**	>300 ± 31.82	2.12 ± 0.94	1.69 ± 1.24	3.00 ± 1.35	3.95 ± 0.09
15	**6**	6.88 ± 0.085	4.68 ± 1.64	1.16 ± 0.32	2.61 ± 0.34	0.84 ± 0.34
16	**7**	3.80 ± 0.28	1.63 ± 0.40	1.37 ± 0.59	2.69 ± 1.3	1.71 ± 0.52
17	**8**	22.71 ± 1.83	1.41 ± 0.79	2.53 ± 1.41	1.69 ± 0.15	10.83 ± 1.40
18	**9**	74.09 ± 5.09	3.03 ± 1.5	1.22 ± 0.64	2.35 ± 1.05	4.11 ± 2.1
19	**10**	15.82 ± 0.97	4.01 ± 0.91	2.93 ± 0.15	5.57 ± 2.01	5.69 ± 1.91
20	paclitaxel	78.88 ± 0.79	0.006 ± 0.0014	4.73 ± 0.83	1.04 ± 0.31	0.013 ± 0.19

[a]All experiments were conducted in triplicate. [b]IC_{50} ± SD (half-maximal inhibitory concentration ± standard deviation) values for all compounds are expressed in micromolar units.

Phytochemicals **5**−**10**, and the well-known anticancer drug, paclitaxel (Taxol), were used as references. Table 3 reports the IC_{50} values (half-maximal inhibitory concentration) of the tested compounds. The stability of compound **11iv** in the cell culture medium has been evaluated by thin-layer chromatographic (TLC) and high-performance liquid chromatography (HPLC) analyses as a selected example. No traces of tyrosol were observed during 48 h, confirming the stability of the ester bond under the reported experimental conditions (see the Supporting Information SI #1−2 and Figures S1−S3).

In the case of the HeLa cell line, artemisinin derivatives were less active than paclitaxel, with an antiproliferative effect comparable to that of artemisinin. The dimer, **11vii**, containing the tyrosol scaffold, showed a remarkable anticancer activity against both SK-MEL24 and RPMI-7951 melanoma cell lines, with IC_{50} values (0.24 and 0.49 μM, respectively) lower than, or comparable to, those of artemisinin and paclitaxel, respectively. Unfortunately, **11vii** was also characterized by a significant activity against the C3PV cell line. The dimer, **11viii**, containing the curcumin scaffold, was active against all melanoma cell lines studied, without any appreciable effect on the C3PV cell.

Note that perillyl alcohol **7** and tyrosol **8** showed higher activity and lower toxicity when incorporated into the artemisinin scaffold, as in the case of hybrids **11iii** (Table 3, entry 6 versus entry 16) and **11ix** (Table 3, entry 12 versus entry 17) against the SK-MEL24 and RPMI-7951 cell lines, respectively.

Compounds **11iv** and **11ix** showed antiproliferative activity against all studied melanoma cell lines, with acceptable tolerability toward the C3PV cell line. They were characterized by a toxicity higher than that of tyrosol **8**, highlighting a different effect of the artemisinin scaffold on the toxicity of the hybrid, depending on the nature of the associated phytochemical.

Artemisinin **1** and the novel artemisinin derivatives, **11iii**−**iv**, **11viii**, and **11ix**, were found to be cancer-selective, being not cytotoxic on normal cell line C3PV. Moreover, compound **11iv** possessed a melanoma-specific cancer selectivity (inactive against HeLa).

As a general trend, curcumin **5** was the most effective phytochemical in the dimer-type derivatives, whereas perillyl alcohol **7** and tyrosol **8** were the most effective in the hybrid-type compounds. Moreover, artesunate appeared to be the most active artemisinin derivative. To obtain information about the mechanism of action of compounds **11iii**−**iv**, **11viii**, and **11ix**, we repeated the cellular assays on the cancer lines in the presence of the iron chelating agent, deferoxamine (DFO),[27,28] able to inhibit the redox activation of the endoperoxide ring.

As reported in Table 4, the presence of DFO significantly lowered the efficacy of artemisinin **1**, confirming the beneficial role of iron in triggering the radical cascade mechanism responsible for the anticancer activity. A similar pathway was observed for compounds **11iv** and **11ix** containing the tyrosol scaffold. Instead, the anticancer activity of perillyl alcohol and curcumin in **11iii** and **11viii** was found to be independent from the presence of iron, suggesting the possibility of an alternative mechanism. Regarding the SK-MEL24 line, the activity of the four synthetic compounds seems to be not influenced by the iron chelation mediated by DFO.

Electron paramagnetic resonance (EPR) analysis was further performed to characterize the radical species formed during the endoperoxide ring opening in the presence of $Fe(II)SO_4$ as a catalyst (for the general procedure see SI #3). Figure 2 shows the EPR spectra of 2-methyl-nitrosopropane (MNP) adducts of artesunate derivatives **11iii**, **11iv**, **11ix**, and **11viii**, recorded as representative active samples (25 °C, t = 0), in comparison with the appropriate reference [that is, the compound and MNP without the Fe(II) salt].

DOI: 10.1021/acsomega.9b02600
ACS Omega 2020, 5, 243−251

Table 4. IC_{50} Values of Compounds 11iii, 11iv, 11viii, and 11ix on the RPMI-7951, SK-MEL3, and SK-MEL24 Cancer Cell Lines in the Presence or Absence of DFO[a,b]

	IC50 ± SD[c]					
	RPMI-7951		SK-MEL3		SK-MEL24	
CPD	without DFO	with DFO	without DFO	with DFO	without DFO	with DFO
1	3.62 ± 1.6	28.97 ± 2.8	3.43 ± 0.8	>300 ± 3.8	8.66 ± 0.9	27.8 ± 3.4
3	1.08 ± 0.6	1.09 ± 0.9	>300 ± 5.6	>300 ± 4.5	0.82 ± 0.05	0.90 ± 0.02
11iii	2.35 ± 0.9	2.95 ± 0.7	5.24 ± 0.2	5.6 ± 0.6	0.06 ± 0.01	0.16 ± 0.04
11iv	8.34 ± 2.7	81.7 ± 5.7	2.33 ± 0.09	24.5 ± 1.3	2.32 ± 0.9	2.5 ± 0.6
11viii	1.37 ± 0.9	1.18 ± 0.7	2.41 ± 0.8	3.8 ± 0.8	2.54 ± 0.5	3.3 ± 0.8
11ix	0.09 ± 0.05	24.5 ± 2.1	2.66 ± 0.9	10.5 ± 2.3	1.5 ± 0.04	6.0 ± 1.5

[a]All experiments were conducted in triplicate. [b]The treatment time was 24 hours for all experiments. [c]IC_{50} ± SD (half-maximal inhibitory concentration ± standard deviation) values for all compounds are expressed in micromolar units.

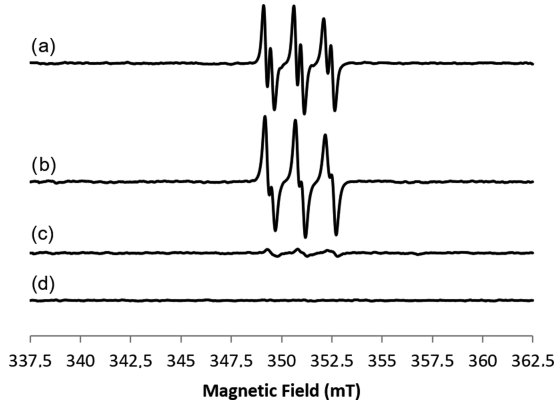

Figure 2. Room-temperature CW-EPR spectra of (a) **11iv**, (b) **11iii**, (c) **11ix**, and (d) blank, all recorded at t = 0 in the presence of the spin trap MNP. Experimental conditions: ν = 9.86GHz, 0.1 mT modulation amplitude, and 0.63 mW microwave power.

The EPR spectra of hybrid derivatives **11iv** and **11iii** (Figure 2, lines a and b, respectively) show the same line shape with g_{iso} = 2.006 ± 0.0001, A_N = 1.49 ± 0.1mT, and A_H = 0.3±0.01mT. In accordance with the EPR results previously reported for artemisinin,[29] the magnetic parameters of artesunate derivatives **11iv** and **11iii** clearly identified the formation of a secondary C-centered radical.[30] The EPR signal decreased over time (Figures S4 and S5, respectively). For hybrid derivative **11ix** (line c), the C-centered radical is present with a low intensity at t = 0, being stable during all recorded times (see Figure S6). Unexpectedly, in the case of dimer derivative **11viii** (Figure S8), no radical formation was detected (only at t = 90 min a very weak signal appeared, but it was no more present at t = 150 min). Note that artesunate alone showed a different behavior with respect to hybrids **11iv** and **11iii** (Figure S7).

Even though a direct correlation between the in vitro EPR analysis of artemisinin derivatives and the in-cell anticancer activity cannot be made, in the case of compound **11iv**, the formation of a secondary C-centered radical was in accordance with the role suggested for this type of intermediate in the biological activity of artemisinin.[29] Moreover, the biological activity of **11iv** dropped after treatment with DFO, whereas that of compound **11viii**, deprived of an EPR signal, was unaffected by the DFO treatment.

CONCLUSIONS

A library of novel derivatives with hybrid and dimer structures were synthesized by coupling between artesunate and dihydroartemisinin, with six phytochemicals, curcumin, eugenol, perillyl alcohol, tyrosol, and α- and δ-tocopherol. Among the novel derivatives, **11iii–iv**, **11viii**, and **11ix** showed a significant and selective anticancer activity. Moreover, the hybrid derivative, **11iv**, was characterized by a specific melanoma selectivity, being inactive against HeLa cells. This compound showed the formation of a secondary C-centered radical in the EPR analysis. DFO studies on the role of endoperoxide ring opening in the antimelanoma activity of **11iv** confirmed the relevant role of the formation of radical intermediates in the biological effect. Surprisingly, the anticancer activity of dimer **11viii** was not dependent on the formation of radical species, leaving open the possibility for other mechanisms to be operative. Further studies aimed at the determination of topoisomerase I as a possible target for the activity of these novel derivatives, as well as transcriptome comparison with other efficient antimelanoma drugs are still ongoing.

EXPERIMENTAL SECTION

Chemistry: General Part. All reactions were performed in flame-dried glassware under a nitrogen atmosphere. Reagents were obtained from commercial suppliers (Sigma-Aldrich Srl, Milan, Italy) and used without further purification. TLC chromatography was performed on precoated aluminum silica gel SIL G/UV254 plates (Macherey-Nagel & Co.). The detection occurred via fluorescence quenching or development in a molybdato phosphate solution (10% in EtOH). Merck silica gel 60 was used for flash chromatography (23–400 mesh). All products were dried in high vacuum (10^{-3} mbar). ^{1}H NMR and ^{13}C NMR spectra were measured on a Bruker Avance DRX400 (400 MHz/100 MHz) and on a Bruker Avance DPX200 (200 MHz/50 MHz) spectrometers. Chemical shifts for protons are reported in parts per million (δ scale) and internally referenced to the CD_3OD or $CDCl_3$ signal at δ 3.33 and 7.28 ppm, respectively. Mass spectral (MS) data were obtained using an Agilent 1100 LC/MSD VL system (G1946C) with a 0.4 mL/min flow rate using a binary solvent system of 95:5 methyl alcohol/water. UV detection was monitored at 254 nm. Mass spectra were acquired in positive and negative mode scanning over the mass range. Elemental analyses (C, H, N) were performed in house. Artemisinin, dihydroartemisinin, and artesunate were obtained from Lachifarma s.r.l. (Zollino (LE), Italy).

*General Procedure for the Synthesis of Derivatives **11i–vii**.* To a solution of artesunate (0.52 mmol, 1.0 equiv) in dry CH_2Cl_2 (3.0 mL), DCC (0.52 mmol, 1.0 equiv) and DMAP (0.16 mmol, 30 mol %) were added at room temperature. After the addition of the opportune phytochemical (0.52 mmol, 1.0 equiv), the reaction mixture was slowly stirred overnight (18 h) under a N_2 atmosphere. The precipitated dicyclohexylurea was removed by filtration, and the solvent was removed under reduced pressure. The residue was purified by gradient column chromatography (hexane/EtOAc 1:1, 1:2).

DOI: 10.1021/acsomega.9b02600
ACS Omega 2020, 5, 243–251

*Compound **11i**.*

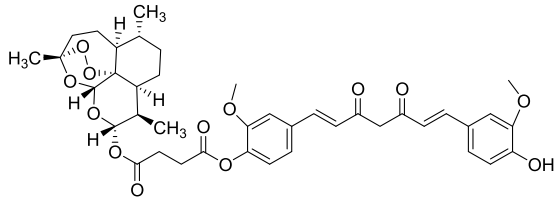

Yield = 50%. R_f = 0.36 (hexane/EtOAc 1:2, molybdato phosphate). ^{1}H NMR ($CDCl_3$, 400 MHz): δ = 7.62 (d, 1H, J = 7.2 Hz), 7.58 (d, 1H, J = 7.2 Hz), 7.16−7.06 (m, 5H), 6.94 (d, 1H, J = 8.0 Hz), 6.57−6.46 (m, 2H), 5.85−5.81 (m, 2H), 5.46 (s, 1H), 3.95 (s, 3H), 3.88 (s, 3H), 2.98−2.92 (m, 2H), 2.88−2.84 (m, 2H), 2.62−2.57 (m, 1H), 2.43−2.34 (m, 1H), 2.04−1.47 (m, 6H), 1.45 (s, 3H), 1.41−1.30 (m, 2H), 1.08−1.00 (m, 1H), 0.98 (d, 3H, J = 5.7 Hz), 0.86 (d, 3H, J = 7.2 Hz) ppm. ^{13}C NMR ($CDCl_3$, 100 MHz): δ = 184.5, 183.3, 183.1, 181.9, 171.2, 170.9, 170.1, 151.4, 148.1, 147.9, 146.9, 141.1, 140.6, 134.1, 124.3, 123.0, 122.1, 114.9, 109.7, 104.5, 92.4, 92.3, 80.1, 60.4, 55.9, 51.6, 45.2, 37.3, 36.2, 34.1, 31.8, 29.1, 28.8, 25.9, 24.6, 22.1, 22.0, 21.0 20.2 12.0 ppm. MS (ESI): m/z for $[C_{40}H_{45}O_{13}]^-$: 733. Anal. calcd for $C_{40}H_{46}O_{13}$: C, 65.38; H, 6.31; O, 28.31; found: C, 65.34; H, 6.30; O, 28.28.

*Compound **11ii**.*

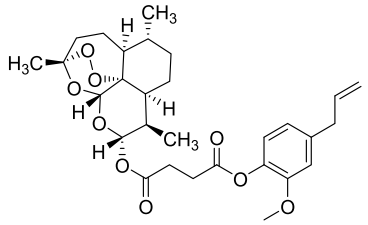

Yield = 49%. R_f = 0.70 (hexane/EtOAc 4:1, molybdato phosphate). ^{1}H NMR ($CDCl_3$, 200 MHz): δ = 6.95 (d, 1H, J = 8.0 Hz), 6.74−6.70 (m, 2H), 5.99−5.85 (m, 1H), 5.77 (d, 1H, J = 9.8 Hz), 5.42 (s, 1H), 5.08 (d, 1H, J = 6.8 Hz), 5.02 (s, 1H), 3.77 (s, 3H), 3.34 (d, 2H, J = 6.6 Hz), 2.96−2.76 (m, 4H), 2.60−2.41 (m, 1H), 2.04−1.47 (m, 6H), 1.41 (s, 3H), 1.30−1.05 (m, 4H), 0.93 (d, 3H, J = 5.2 Hz), 0.81 (d, 3H, J = 7.2 Hz) ppm. ^{13}C NMR ($CDCl_3$, 50 MHz): δ = 170.9, 170.4, 138.9, 137.9, 137.0, 122.5, 120.6, 116.1,112.7, 104.4, 92.2, 91.5, 80.1, 55.8, 51.6, 45.2, 40.0, 37.3, 36.2, 34.1, 31.8, 29.3, 28.7, 25.9, 24.6, 21.9, 20.2, 12.0 ppm. MS (ESI): m/z for $[C_{29}H_{39}O_9]^+$: 532. Anal. calcd for $C_{29}H_{39}O_9$: C, 65.64; H, 7.22; O, 27.14; found: C, 65.67; H, 7.24; O, 27.16.

*Compound **11iii**.*

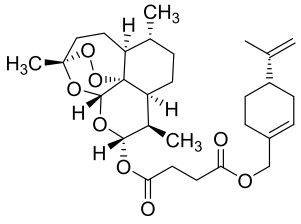

Yield = 82%. R_f = 0.67 (hexane/EtOAc 4:1, molybdato phosphate). ^{1}H NMR ($CDCl_3$, 200 MHz): δ = 5.75 (d, 1H, J = 9.8 Hz), 5.72−5.71 (m, 1H), 5.39 (s, 1H), 4.68−4.66 (m, 2H), 4.43 (s, 2H), 2.71−2.61 (m, 4H), 2.60−2.41 (m, 1H), 2.39−2.25 (m, 1H), 2.12−1.76 (m, 10H), 1.69 (s, 3H), 1.63−1.41 (m, 3H), 1.38 (s, 3H), 1.35−1.17 (m, 3H), 1.16−0.94 (m, 1H), 0.92 (d, 3H, J = 5.6 Hz), 0.81 (d, 3H, J = 7.2 Hz) ppm. ^{13}C NMR ($CDCl_3$, 50 MHz): δ = 171.9, 171.0, 149.5, 132.4, 125.9, 108.7, 104.4, 92.1, 91.5, 80.0, 68.7, 51.5, 45.2, 40.7, 37.2, 34.1, 31.8, 30.4, 29.2, 28.9, 27.2, 26.3, 26.1, 25.8, 24.5, 21.9, 20.7, 20.2, 12.0 ppm. MS (ESI): m/z for $[C_{29}H_{43}O_8]^+$: 519. Anal. calcd for $C_{29}H_{42}O_8$: C, 67.16; H, 8.16; O, 24.68; found: C, 67.17; H, 8.14; O, 24.66.

*Compound **11iv**.*

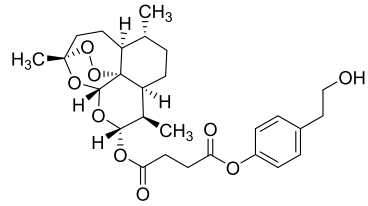

Yield = 53%. R_f = 0.50 (hexane/EtOAc 4:1, molybdato phosphate). ^{1}H NMR ($CDCl_3$, 200 MHz): δ = 7.17 (d, 2H, J = 8.6 Hz), 6.98 (d, 1H, J = 8.6 Hz), 5.78 (d, 1H, J = 10.0 Hz), 5.40 (s, 1H), 3.76 (t, 2H, J = 6.6 Hz), 2.85−2.75 (m, 6H), 2.55−2.51 (m, 1H), 2.34−2.25 (m, 1H), 2.02−1.41 (m, 6H), 1.41 (s, 3H), 1.35−0.99 (m, 4H), 0.91 (d, 3H, J = 5.4 Hz), 0.80 (d, 3H, J = 7.2 Hz) ppm. ^{13}C NMR ($CDCl_3$, 50 MHz): δ = 170.9, 170.8, 149.1, 136.3, 129.9, 121.5, 104.5, 92.3, 91.5, 80.1, 63.5, 51.5, 45.2, 38.5, 37.2, 36.2, 34.1, 31.8, 29.2, 29.0, 25.8, 24.6, 21.9, 20.2, 14.2, 12.0 ppm. MS (ESI): m/z for $[C_{27}H_{36}O_9Na]^+$: 528. Anal. calcd for $C_{27}H_{36}O_9$: C, 64.27; H, 7.19; O, 28.54; found: C, 64.28; H, 7.20; O, 28.55.

*Compound **11v**.*

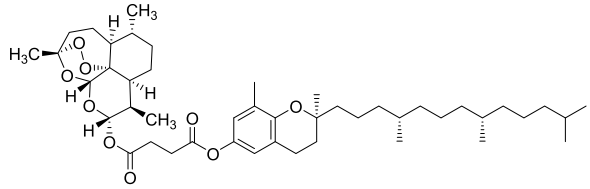

Yield = 72%. R_f = 0.19 (hexane/EtOAc 9:1, molybdato phosphate). ^{1}H NMR ($CDCl_3$, 200 MHz): δ = 6.65−6.58 (m, 2H), 5.80 (d, 1H, J = 9.8 Hz), 5.42 (s, 1H), 2.91−2.60 (m, 8H), 2.58−2.45 (m, 1H), 2.36−2.21 (m, 1H), 2.04 (s, 3H), 2.02−1.05 (m, 25H), 1.41 (s, 3H), 1.23 (s, 3H), 0.94 (d, 3H, J = 5.8 Hz), 0.89−0.80 (m, 18H) ppm. ^{13}C NMR ($CDCl_3$, 50 MHz): δ = 171.3, 170.9, 149.7, 142.3, 127.2, 121.0, 120.8, 118.9, 104.4, 92.2, 91.5, 80.0, 51.5, 45.2, 40.1, 39.3, 37.4, 37.2, 34.1, 32.7, 32.6, 31.7, 29.2, 28.9, 25.9, 24.6, 24.4, 24.2, 22.7, 22.6, 22.4, 22.0, 21.0, 20.2, 19.7, 19.6, 16.0, 12.4 ppm. MS (ESI): m/z for $[C_{46}H_{73}O_9]^+$: 769. Anal. calcd for $C_{46}H_{72}O_9$: C, 71.84; H, 9.44; O, 18.72; found: C, 71.87; H, 9.43; O, 18.75.

*Compound **11vi**.*

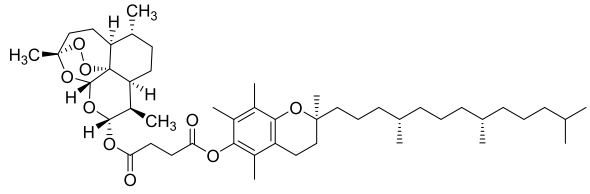

Yield = 60%. R_f = 0.27 (hexane/EtOAc 9:1, molybdato phosphate). ^{1}H NMR ($CDCl_3$, 200 MHz): δ = 5.80 (d, 1H, J = 9.8 Hz), 5.42 (s, 1H), 2.96−2.70 (m, 4H), 2.56−2.49 (m, 3H), 2.45−2.21 (m, 1H), 2.36−2.21 (m, 1H), 2.02 (s, 3H), 1.99 (s, 3H), 1.95 (s, 3H), 1.87−1.01 (m, 8H), 0.95−0.81 (m, 18H) ppm. ^{13}C NMR ($CDCl_3$, 50 MHz): δ = 170.9, 170.7, 149.4, 140.5, 126.7, 124.9, 122.9, 117.3, 104.4, 92.3, 91.5, 80.0, 75.0,

DOI: 10.1021/acsomega.9b02600
ACS Omega 2020, 5, 243−251

51.6, 45.2, 39.4, 37.4, 37.3, 37.2, 36.2, 34.1, 32.8, 32.7, 31.8, 29.2, 27.9, 25.9, 24.8, 24.4, 22.7, 22.6, 22.0, 21.0, 20.2, 19.8, 19.7, 12.9, 12.1, 11.8 ppm. MS (ESI): m/z for $[C_{48}H_{76}O_9]^+$: 784. Anal. calcd for $C_{46}H_{72}O_9$: C, 72.33; H, 9.61; O, 18.06; found: C, 72.31; H, 9.62; O, 18.05.

*General Procedure for the Synthesis of Derivatives **11vii** and **11viii**:* To a solution of artesunate (0.52 mmol, 1.0 equiv) in dry CH_2Cl_2 (3.0 mL), DCC (1.04 mmol, 2.0 equiv) and DMAP (0.32 mmol, 60 mol %) were added at room temperature. After the addition of the opportune phytochemical (1.04 mmol, 2.0 equiv), the reaction mixture was slowly stirred overnight (18 h) under a N_2 atmosphere. The precipitated dicyclohexylurea was removed by filtration, and the solvent was removed under reduced pressure. The residue was purified by gradient column chromatography (hexane/EtOAc 1:1, 1:2).

*Compound **11vii**.*

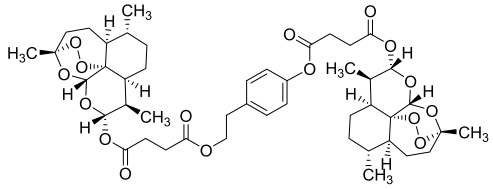

Yield = 47%. R_f = 0.50 (hexane/EtOAc 9:1, molybdato phosphate). ^{1}H NMR ($CDCl_3$, 200 MHz): δ = 7.00 (d, 2H, J = 8.6 Hz), 6.81 (d, 2H, J = 8.6 Hz), 5.59 (d, 1H, J = 6.4 Hz), 5.54 (d, 1H, J = 6.4 Hz), 5.24 (s, 1H), 5.22 (s, 1H), 4.05 (t, 2H, J = 7.0 Hz), 2.74−2.57 (m, 6H), 2.50−2.25 (m, 6H), 2.20−2.06 (m, 2H), 1.84−1.19 (m, 12H), 1.18 (s, 3H), 1.17 (s, 3H), 1.11−0.82 (m, 8H), 0.74 (d, 6H, J = 5.8 Hz), 0.64−0.60 (m, 6H) ppm. ^{13}C NMR ($CDCl_3$, 50 MHz): δ = 171.7, 170.8, 170.7, 170.5, 149.16, 135.2, 129.7, 129.6, 121.4, 104.1, 92.1, 92.0, 91.3, 79.9, 64.8, 51.4, 48.4, 45.0, 37.0, 36.0, 34.2, 33.9, 33.7, 31.6, 30.6, 30.3, 29.8, 29.4, 29.0, 28.9, 28.8, 28.6, 25.6, 24.8, 24.4, 21.7, 20.0, 11.8, 11.7 ppm. MS (ESI): m/z calcd for $[C_{45}H_{61}O_{16}]^+$: 856. Anal. calcd for $C_{45}H_{60}O_{16}$: C, 63.07; H, 7.06; O, 29.87; found: C, 63.08; H, 7.05; O, 29.85.

*Compound **11viii**.*

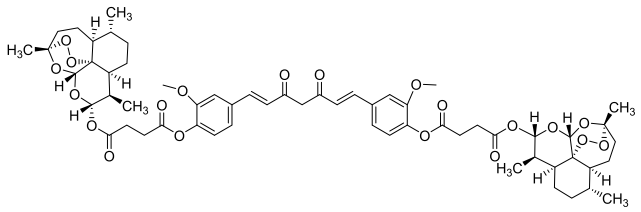

Yield = 59%. R_f = 0.39 (hexane/EtOAc 9:1, molybdato phosphate). ^{1}H NMR ($CDCl_3$, 200 MHz): δ = 7.57 (d, 2H, J = 15.8 Hz), 7.13−7.02 (m, 6H), 6.52 (d, 2H, J = 15.8 Hz), 5.83−5.76 (m, 2H), 5.40 (s, 2H), 3.82 (s, 6H), 2.97−2.76 (m, 8H), 2.59−2.48 (m, 2H), 2.42−2.26 (m, 2H), 2.12−1.50 (m, 12H), 1.46 (s, 6H), 1.39−0.99 (m, 8H), 0.91 (d, 6H, J = 5.4 Hz), 0.74 (d, 6H, J = 18.2 Hz) ppm. ^{13}C NMR ($CDCl_3$, 50 MHz): δ = 183.1, 170.8, 170.1, 151.3, 141.2, 139.9, 134.0, 124.3, 123.3, 121.1, 111.4, 104.4, 101.8, 92.3, 91.5, 80.1 60.3, 55.9, 51.5, 45.2, 37.2, 36.2, 34.1, 31.8, 29.2, 28.7, 25.9, 25.0, 24.6, 22.0, 20.2, 14.2, 12.0 ppm.MS (ESI): m/z for $[C_{59}H_{73}O_{20}]^+$: 1101. Anal. calcd for $C_{59}H_{72}O_{20}$: C, 64.35; H, 6.59; O, 29.06; found: C, 64.31; H, 6.62; O, 29.05.

*Procedure for the Synthesis of Derivative **11ix**.* To a solution of artesunic acid (0.52 mmol, 1.0 equiv) in dry DMF (3.0 mL), K_2CO_3 (1.04 mmol, 2.0 equiv) and 4-hydroxyphenethyl bromide (0.52 mmol, 1.0 equiv) were added at room temperature. The reaction mixture was warmed at 90 °C and stirred overnight (18 h) under a N_2 atmosphere. After this time, the precipitate was removed by filtration, and the solution was diluted with H_2O (20 mL) and extracted with EtOAc (3 × 25 mL). The organic phase was washed with brine dried over Na_2SO_4, filtered, and concentrated under reduced pressure. The crude product was purified by column chromatography (hexane/EtOAc 1:1).

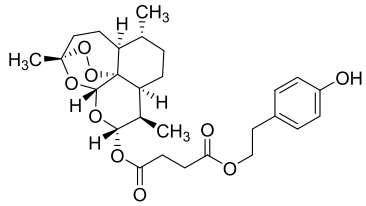

Yield = 46%. R_f = 0.33 (hexane/EtOAc 4:1, molybdato phosphate). ^{1}H NMR ($CDCl_3$, 200 MHz): δ = 7.04 (d, 2H, J = 8.4 Hz), 6.76 (d, 2H, J = 8.4 Hz), 5.75 (d, 2H, J = 9.8 Hz), 5.42 (s, 2H), 4.22 (t, 2H, J = 7.0 Hz), 2.83 (d, 2H, J = 7.0 Hz), 2.63−2.48 (m, 4H), 2.35−2.28 (m, 2H), 1.97−1.42 (m, 6H), 1.41 (s, 3H), 1.27−0.99 (m, 4H), 0.91 (d, 3H, J = 3.8 Hz), 0.80 (d, 3H, J = 7.0 Hz) ppm. ^{13}C NMR ($CDCl_3$, 50 MHz): δ = 172.0, 171.1, 151.2, 130.0, 129.6, 115.5, 104. 6, 92.2, 91.5, 80.2, 65.4, 51.5, 45.2, 37.3, 36.2, 34.1, 34.0, 33.2, 31.8, 29.7, 29.1, 28.9, 28.0, 25.9, 24.6, 22.7, 22.0, 21.0, 20.2, 14.2, 13.2, 12.0 ppm. MS (ESI): m/z for $[C_{27}H_{35}O_9]^-$: 503. Anal. calcd for $C_{27}H_{36}O_9$: C, 64.27; H, 7.19; O, 28.54; found: C, 64.29; H, 7.18; O, 28.53.

*Procedure for the Synthesis of Derivative **11x**.* To a solution of dihydroartemisinin (0.52 mmol, 1.0 equiv) in dry DMF (3.0 mL), K_2CO_3 (1.04 mmol, 2.0 equiv) and 4-hydroxyphenethyl bromide (0.52 mmol, 1.0 equiv) were added at room temperature. The reaction mixture was warmed at 90 °C and stirred overnight (18 h) under a N_2 atmosphere. After this time, the precipitate was removed by filtration, and the solution was diluted with H_2O (20 mL) and extracted with EtOAc (3 × 25 mL). The organic phase was washed with brine dried over Na_2SO_4, filtered, and concentrated under reduced pressure. The crude product was purified by column chromatography (hexane/EtOAc 1:1).

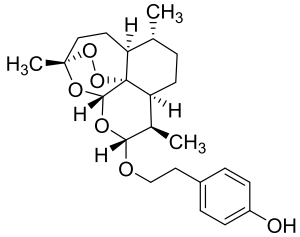

Yield = 53% (a mixture of α and β isomers). R_f = 0.27 (hexane/EtOAc 9:1, molybdato phosphate). ^{1}H NMR ($CDCl_3$, 200 MHz): δ = 7.06−7.00 (m, 2H), 6.76−6.69 (m, 2H), 5.11 (s, 1H), 4.74 (d, J = 3.4 Hz), 4.04−3.92 (m, 1H), 3.57−3.46 (m, 1H), 2.80−2.72 (m, 2H), 2.56−2.51 (m, 1H), 2.37−2.30 (m, 1H), 2.29−1.41 (m, 6H), 1.39 (s, 3H), 1.37−0.91 (m, 4H), 0.90−0.85 (m, 3H), 0.82 (d, 3H, J = 7.4 Hz) ppm. ^{13}C NMR ($CDCl_3$, 50 MHz): δ = 154.2, 131.2, 130.9, 130.0, 115.1, 115.0, 104.1, 103.2, 102.8, 101.7, 88.8, 87.9, 81.1, 69.5, 69.1, 52.4, 51.9, 46.2, 44.2, 39.4, 37.2, 37.1, 36.5, 36.4,

DOI: 10.1021/acsomega.9b02600
ACS Omega 2020, 5, 243−251

35.4, 34.6, 34.4, 31.4, 30.9, 26.1, 25.9, 24.6, 24.2, 20.3, 20.0, 19.5, 12.9 ppm. MS (ESI): m/z for $[C_{23}H_{31}O_6]^-$: 403. Anal. calcd for $C_{23}H_{32}O_6$: C, 68.29; H, 7.97; O, 23.73; found: C, 68.230; H, 7.99; O, 23.74.

Biological Part. *Cell Culture Condition.* The C3PV cell line is a primary human fibroblast grown according to Botta et al.[31] SK-MEL3, SK-MEL24 and RPMI-7951 are three different metastatic melanoma cancer cell lines. SK-MEL3 was grown in McCoy's medium supplemented with 15% fetal bovine serum (FBS), penicillin (100 U/mL), and streptomycin (1 mg/mL). SK-MEL24 and RPMI-7951 were grown in Eagle's minimum essential medium containing 15 and 10% FBS, respectively, penicillin (100 U/mL), and streptomycin (1 mg/mL). All cell lines were maintained at 37 °C in a humidified atmosphere (95%) and 5% CO_2.

Treatment Protocol: General Procedure. To study the effect of artemisinin and its derivatives on cell viability, the C3PV, SK-MEL3, SK-MEL24, and RPMI-7951 cell lines were seeded in 96-well plates (6000 cells/well in 100 μL of medium) and incubated overnight to allow cell adherence. Afterward, the medium was replaced with fresh medium containing the appropriate dose of compounds. Artemisinin and its derivatives were used in a range of 0.01 to 1 μM for 24 h. The analyses of cell viability were done at the end of treatment. The assays were performed in quadruplicate for both treatments.

Treatment Protocol for DFO Assay. To study the mechanism of action of artemisinin and compounds **11iii**, **11iv**, **11viii**, and **11ix**, the SK-MEL3, SK-MEL24 and RPMI-7951 cell lines were seeded in 96-well plates (6000 cells/well in 100 μL of medium) and incubated overnight to allow cell adherence. Afterward, the medium was replaced with fresh medium containing DFO (20 μM) for 1 h. Then the appropriate dose of artemisinin and its compounds **11iii**, **11iv**, and **11viii** were added for 24 h. The analyses of cell viability were done at the end of treatment. The assays were performed in quadruplicate for both treatments.

Cell Viability Assay. Cell viability was evaluated using MTT [3-(4,5-dimethylthiazol-2-yl)-2,5-diphenyl-2H-tetrazolium bromide] cell proliferation assay. Briefly, after incubation for 3 h at 37 °C with MTT (0.5 mg/mL), the supernatant was replaced with 100 μL of analysis solution containing 10% sodium dodecyl sulfate and 0.6% acetic acid in dimethyl sulfoxide to dissolve the formazan crystals. Optical density measurements were performed with a scanning spectrophotometer DTX880 Multimode Detector (Beckman Coulter) using a 630 nm (background) and a 570 nm filter.

Statistical Analysis. The IC_{50} values were determined by nonlinear regression using the program, graphpad prism 6. The SI values were calculated using the formula

$$IC_{50}(\text{treated wt cell line})/IC_{50}(\text{treated tumor cell line})$$

■ ASSOCIATED CONTENT

Supporting Information

The Supporting Information is available free of charge at https://pubs.acs.org/doi/10.1021/acsomega.9b02600.

Stability of compound **11iv** by TLC and HPLC analyses; HPLC analysis of compound **11iv** (Figure S1); HPLC analysis of tyrosol 8 (Figure S2); HPLC analysis of compound **11iv** after 48 h treatment with cell culture medium at room temperature (Figure S3); EPR procedure; EPR spectra of compounds **11iv**, **11iii**, **11ix**, artesunate and **11viii** (Figures S4–S8).

■ AUTHOR INFORMATION

Corresponding Authors

*E-mail: lorenzo.botta@unitus.it (L.B.).
*E-mail: saladino@unitus.it (R.S.).

ORCID

Bruno M. Bizzarri: 0000-0001-7085-5432
Raffaele Saladino: 0000-0002-4420-9063

Author Contributions

The manuscript was written through contributions of all authors. All authors have given approval to the final version of the manuscript.

Notes

The authors declare no competing financial interest.

■ ACKNOWLEDGMENTS

This article is dedicated to Dr. Luigi Villanova, ex-President of Lachifarma, for his pioneering studies on artemisinin as an antimelanoma agent. The article is published with the contribution of MIUR Ministero dell'Istruzione, dell'Università della Ricerca Italiano, project PRIN 2017, ORIGINALE CHEMIAE in Antiviral Strategy—Origin and Modernization of Multi-Component Chemistry as a Source of Innovative Broad Spectrum Antiviral Strategy, cod. 2017BMK8JR.

■ REFERENCES

(1) Tu, Y. The discovery of artemisinin (qinghaosu) and gifts from Chinese medicine. *Nat. Med.* **2011**, *17*, 1217–1220.

(2) Posner, G. H. Antimalarial peroxides in the qinghaosu (artemisinin) and yingzhaosu families. *Expert Opin. Ther. Pat.* **1998**, *8*, 1487–1493.

(3) Li, Y.; Wu, Y. L. An over four millennium story behind Qinghaosu (artemisinin): a fantastic antimalarial drug from a traditional Chinese herb. *Curr. Med. Chem.* **2003**, *10*, 2197–2230.

(4) Dhingra, V.; Vishweshwar, R. K.; Lakshmi, N. M. Current status of artemisinin and its derivatives as antimalarial drugs. *Life Sci.* **2000**, *66*, 279–300.

(5) Lai, H. C.; Singh, N. P.; Sasaki, T. Development of artemisinin compounds for cancer treatment. *Invest. New Drugs* **2013**, *31*, 230–246.

(6) Efferth, T.; Dunstan, H.; Sauerbrey, A.; Miyachi, H.; Chitambar, C. R. The anti-malarial artesunate is also active against cancer. *Int. J. Oncol.* **2001**, *18*, 767–773.

(7) Efferth, T. Mechanistic perspectives for 1,2,4-trioxanes in anticancer therapy. *Drug Resist. Updates* **2005**, *8*, 85–97.

(8) Kelter, G.; Steinbach, D.; Konkimalla, V. B.; Tahara, T.; Taketani, S.; Fiebig, H. H.; Efferth, T. Role of transferrin receptor and ABC transporters ABCB6 and ABCB7 for resistence and differentiation of tumors cells towards artesunate. *PLoS One* **2007**, *2*, No. e798.

(9) Butler, A. R.; Gilbert, B. C.; Hulme, P.; Irvine, L. R.; Renton, L.; Whitwood, A. C. EPR Evidence for the Involvement of Free Radicals in the Iron-Catalysed Decomposition of Qinghaosu (Artemisinin) and Some Derivatives; Antimalarial Action of Some Polycyclic Endoperoxides. *Free Radical Res.* **1998**, *28*, 471–476.

(10) Francis, S. E.; Sullivan, D. J., Jr.; Goldberg, D. E. Hemoglobin metabolism in the malaria parasite Plasmodium falciparum. *Annu. Rev. Microbiol.* **1997**, *51*, 97–123.

(11) (a) Tietze, L. F.; Bell, H. P.; Chandrasekhar, S. Natural Product Hybrids as New Leads for Drug Discovery. *Angew. Chem., Int. Ed.* **2003**, *42*, 3996–4028. (b) Zhang, N.; Yu, Z.; Yang, X.; Hu, P.; He, Y. Synthesis of novel ring-contracted artemisinin dimers with potent anticancer activities. *Eur. J. Med. Chem.* **2018**, *150*, 829–840.

DOI: 10.1021/acsomega.9b02600
ACS Omega 2020, 5, 243–251

(c) Letis, A. S.; Seo, E. J.; Nikolaropoulos, S. S.; Efferth, T.; Giannis, A.; Fousteris, M. A. Synthesis and cytotoxic activity of new artemisinin hybrid molecules against human leukemia cells. *Bioorg. Med. Chem.* **2017**, *25*, 3357−3367. (d) Singh, N. P.; Lai, H. C.; Park, J. S.; Gerhardt, T. E.; Kim, B. J.; Wang, S.; Sasaki, T. Effects of artemisinin dimers on rat breast cancer cells in vitro and in vivo. *Anticancer Res.* **2011**, *31*, 4111−4114.

(12) Fröhlich, T.; Reiter, C.; Saeed, M. E. M.; Hutterer, C.; Hahn, F.; Leidenberger, M.; Friedrich, O.; Kappes, B.; Marschall, M.; Efferth, T.; Tsogoeva, S. B. Synthesis of Thymoquinone−Artemisinin Hybrids: New Potent Antileukemia, Antiviral, and Antimalarial Agents. *ACS Med. Chem. Lett.* **2018**, *9*, 534−539.

(13) Artemisinin derivatives for the treatment of melanoma WO2009/043538.

(14) Surh, Y. J. Cancer Chemoprevention with dietary phytochemicals. *Nat. Rev. Cancer* **2003**, *3*, 768−780.

(15) Garbe, C.; Eigentler, T. K.; Keilholz, U.; Hauschild, A.; Kirkwood, J. M. Systematic review of medical treatment in melanoma: current status and future prospects. *Oncologist* **2011**, *16*, 5−24.

(16) Mirzaei, H.; Naseri, G.; Rezaee, R.; Mohammadi, M.; Bakazemi, Z.; Mirzaei, H. R.; Salehi, H.; Peyvandi, M.; Pawelek, J. M.; Sahebkar, A. Curcumin: A new candidate for melanoma therapy? *Int. J. Cancer* **2016**, *139*, 1683−1695.

(17) Ghosh, R.; Nadiminty, N.; Fitzpatrick, J. E.; Alworth, W. L.; Slaga, T. J.; Kumar, A. P. Eugenol Causes Melanoma Growth Suppression through Inhibition of E2F1 Transcriptional Activity. *J. Biol. Chem.* **2005**, *280*, 5812−5819.

(18) Ottino, P.; Duncan, J. R. Effect of α-Tocopherol Succinate on Free Radical and Lipid Peroxidation Levels in BL6 Melanoma Cells Free Radical Biology and Medicine. *Free Radical Biol. Med.* **1997**, *22*, 1145−1151.

(19) Mijatovic, S. A.; Timotijevic, G. S.; Miljkovic, D. M.; Radovic, J. M.; Maksimovic-Ivanic, D. D.; Dekanski, D. P.; Stosic-Grujicic, S. D. Multiple antimelanoma potential of dry olive leaf extract. *Int. J. Cancer* **2011**, *128*, 1955−1965.

(20) Rasheed, S. A.; Efferth, T.; Asangani, I. A.; Allgayer, H. First evidence that the antimalarial drug artesunate inhibits invasion and *in vivo* metastatis in lung cancer by targeting essential extracellular proteases. *Int. J. Cancer* **2010**, *127*, 1475−1485.

(21) Soomro, S.; Langenberg, T.; Mahringer, A.; Konkimalla, V. B.; Horwedel, C.; Holenya, P.; Brand, A.; Cetin, C.; Fricker, G.; Dewerchin, M.; Carmeliet, P.; Conway, E. M.; Jansen, H.; Efferth, T. Design of novel artemisinin-like derivates with cytotoxic and antiangiogenic properties. *J. Cell. Mol. Med.* **2011**, *15*, 1122−1135.

(22) Konkimalla, V. B.; McCubrey, J. A.; Efferth, T. The role of downstream signalling pathways of the epidermal growth factor receptors for Artesunate's activity in cancer cells. *Curr. Cancer Drug Targets* **2009**, *9*, 72−80.

(23) Houben, R.; Becker, J. C.; Kappel, A.; Terheyden, P.; Brocker, E. B.; Goetz, R.; Rapp, U. R. Constitutive activation of the Ras-Raf signaling pathway in metastatic melanoma is associated with poor prognosis. *J. Carcinog.* **2004**, *3*, 6.

(24) (a) Olivier, M.; Hollstein, M.; Hainaut, P. TP53 Mutations in Human Cancers: Origins, Consequences, and Clinical Use. *Cold Spring Harbor Perspect. Biol.* **2010**, *2*, No. a001008. (b) Petitjean, A.; Achatz, M. I. W.; Borresen-Dale, A. L.; Hainaut, P.; Olivier, M. TP53 mutations in human cancers: functional selection and impact on cancer prognosis and outcomes. *Oncogene* **2007**, *26*, 2157−2165.

(25) (a) Halachmi, S.; Gilcherest, B. A. Update on genetic events in the pathogenesis of melanoma. *Curr. Opin. Oncol.* **2001**, *13*, 129−136. (b) Pollock, P. M.; Trent, J. M. The genetics of cutaneous melanoma. *Clin. Lab. Med.* **2000**, *20*, 667−690.

(26) (a) Sharma, A.; Trivedi, N. R.; Zimmerman, M. A.; Tuevasan, D. A.; Smith, C. D.; Robertson, G. P. Mutant V599E B-Raf regulates growth and vascular, development of malignant melanoma tumors. *Cancer Res.* **2005**, *65*, 2412−2421. (b) Smalley, K. S. M.; Brafford, P.; Haass, N. K.; Brandner, J. M.; Brown, E.; Herlyn, M. Up-regulated expression of zonula occludens protein-1 in human melanoma associates with N-cadherin and contributes to invasion and adhesion. *Am. J. Pathol.* **2005**, *166*, 1541−1554.

(27) Zuma, N. H.; Smit, F. J.; de Kock, C.; Combrinck, J.; Smith, P. J.; N'Da, D. D. Synthesis and biological evaluation of a series of non-hemiacetal ester derivatives of artemisinin. *Eur. J. Med. Chem.* **2016**, *122*, 635−646.

(28) Ooko, E.; Saeed, M. E.; Kadioglu, O.; Sarvi, S.; Colak, M.; Elmasaoudi, K.; Janah, R.; Greten, H. J.; Efferth, T. Artemisinin derivatives induce iron-dependent cell death (ferroptosis) in tumor cells. *Phytomedicine* **2015**, *22*, 1045−1054.

(29) Posner, G. H.; Wang, D.; Cumming, J. N.; Oh, C. H.; French, A. N.; Bodley, A. L.; Shapiro, T. A. Further evidence supporting the importance of and the restrictions on a carbon-centered radical for high antimalarial activity of 1,2,4-trioxanes like artemisinin. *J. Med. Chem.* **1995**, *38*, 2273−2275.

(30) Alberti, A.; Macciantelli, D. Spin Trapping. In *Electron Paramagnetic Resonance − a Practitioner's Toolkit*; Brustolon, M.; Giamello, E., Eds.; Wiley: Hoboken, 2009; pp 287−323.

(31) Botta, L.; Filippi, S.; Bizzarri, B. M.; Meschini, R.; Caputo, M.; Proietti-De-Santis, L.; Iside, C.; Nebbioso, A.; Gualandi, G.; Saladino, R. Oxidative nucleophilic substitution selectively produces cambinol derivatives with antiproliferative activity on bladder cancer cell lines. *Bioorg. Med. Chem. Lett.* **2019**, *29*, 78−82.

DOI: 10.1021/acsomega.9b02600
ACS Omega 2020, 5, 243−251